

Spatial and velocity coincidence of 4765- and 1720-MHz OH masers in two star-forming regions Cep A and W75N

A. Niezurawska,¹ M. Szymczak,¹ R.J. Cohen² and A.M.S. Richards²

¹*Toruń Centre for Astronomy, Nicolaus Copernicus University, Gagarina 11, 87-100 Toruń, Poland*

²*Jodrell Bank Observatory, University of Manchester, Macclesfield, Cheshire SK11 9DL, UK*

Released 2003 Xxxxx XX

ABSTRACT

We present the first maps of 4765-MHz OH masers in two star-forming regions Cepheus A and W75N, made with Multi-Element Radio Linked Interferometer Network. In Cep A the emission has an arc-like structure of size 40 mas with a clear velocity gradient, and lies at the edge of H II region 3b. Over a period of 8 weeks the maser diminished in intensity by a factor of 7 but its structure remained stable. This structure coincides with a newly mapped 1720-MHz maser in Cep A within the positional error, and matches it in velocity. No emission of any other ground state or 4.7-GHz excited OH transitions was detected in the 4765/1720-MHz region. The 1720-MHz line exhibits Zeeman splitting that corresponds to a magnetic field strength of -17.3 mG. In W75N the excited 4765-MHz OH maser has a linear structure of size 45 mas with a well defined velocity gradient, and lies at the edge of H II region VLA 1. This structure coincides in position and velocity with the 1720-MHz masers. We conclude that in both sources the 4765-MHz emission coexists with 1720-MHz emission in the same volume of gas. In such a case the physical conditions in these regions are tightly constrained by the maser-pumping models.

Key words: masers – stars: formation – ISM: molecules – radio lines: ISM – H II regions

1 INTRODUCTION

OH maser emission is an important probe of obscured star-forming regions. The maser lines provide high precision information on the location and velocity of the excited gas and on the physical conditions, notably the magnetic field (e.g. Cohen 1989 and references therein). If more than one OH maser transition is detected from the same compact region then it is possible to better constrain the other physical conditions such as gas temperature and density, the dust temperature, and so on (e.g. Gray et al. 2001 and references therein). However the detection of maser transitions of rotationally excited OH is not very efficient, with current equipment. Among three allowed transitions of the excited ${}^2\Pi_{1/2}$, $J=1/2$ state of OH only the 4765-MHz ($F=1-0$) line is usually seen, but even this is very rare (Cohen, Masheder & Walker 1991; Cohen, Masheder & Caswell 1995; Dodson & Ellingsen 2002). A typical profile of a 4765-MHz source contains a single narrow unpolarized feature of intensity of a few hundred mJy which is usually variable on timescales that can be as short as a few weeks (Smits, Cohen & Hutawarakorn 1998; Smits 2003). In fact several sources have been detected only during episodes of flaring. The two well known star-forming regions Cep A and W75N recently detected in

the 4765-MHz line (Szymczak, Kus & Hrynek 2000) appear to belong to this class of objects that experience flaring.

Cep A is a part of the Cepheus OB3 association at an estimated distance of 725 pc (Blaauw, Hiltner & Johnson 1959). The complex contains clusters of bright far infrared sources (e.g. Goetz et al. 1998), compact radio continuum sources (e.g. Hughes, Cohen & Garrington 1995; Garay et al. 1996; Torrelles et al. 1998) and maser sources of several species seen in many transitions (e.g. Cohen, Rowland & Blair 1984; Migenes, Cohen & Brebner 1992; Torrelles et al. 1998; Argon, Reid & Menten 2000). W75N lies in the molecular cloud complex DR21–W75 at a distance of 2 kpc (Dickel, Dickel & Wilson 1978). Several radio continuum sources (e.g. Hunter et al. 1994; Torrelles et al. 1997) and maser sources (Baart et al. 1986; Torrelles et al. 1997; Hutawarakorn, Cohen & Brebner 2002) are observed. Shortly after the discovery of the excited OH maser flares at 4765 MHz in Cep A and W75N we undertook interferometric observations in order to determine the locations of the masers in these very complex star-forming regions.

Single-dish studies have shown a correlation between 4765- and 1720-MHz OH masers (Cohen et al. 1995), a connection that is supported by high angular resolution studies

Table 1. Details of the MERLIN observations

Source	Date	Transition (MHz)	PHASE-CALIBRATOR		SYNTHESISED BEAM			RMS Noise (mJy b ⁻¹)	
			Name	Flux density (mJy)	HPBW (mas)	P.A. (deg)	Time (h)		
Cep A	04Jan1999*	4765.562	2300+638	250	48×38	-14	10	2.5	
	27Jan1999*	4765.562		200	48×40	-12	10	2	
	01Mar1999**	4660.242			230			5	
		4750.656			250			5	
		4765.562			250	49×43	-11	5	6
	20May1999**	1720.530		130	154×107	-24	7.5	3.5	
16Jun1999**	1720.530		150	143×109	-32	4	6		
W75N	14Apr2000**	4765.562	2005+403	2500	49×45	59	7	3	

Antennas: * Defford, Cambridge, Knockin, Darnhall, Mark II

** Defford, Cambridge, Knockin, Darnhall, Mark II, Tabley

of few selected sources (Palmer, Gardner & Whiteoak 1984; Baudry et al. 1988; Gray et al. 2001). Recent observations at arcsecond resolution by Dodson & Ellingsen (2002) have suggested a stronger association between 6035- and 4765-MHz lines than that between 1720- and 4765-MHz emission. Detailed modelling has shown that various combinations of OH transitions can occur in restricted ranges of conditions in regions of shocked gas (Gray, Doel & Field 1991; Gray, Field & Doel 1992; Pavlakis & Kylafis 1996a; Pavlakis & Kylafis 1996b; Cragg, Sobolev & Godfrey 2002). High angular resolution measurements and simultaneous identification of different OH maser transitions in the same volume of gas can be of a great value in estimating very precisely the local physical conditions and distinguishing between different pumping models.

In this paper we report on multi-frequency observations of OH masers in the two objects. Our aims were to locate with high precision the excited and ground state OH masers and to determine their observational characteristics. The observations demonstrate for the first time the co-propagation of maser emission at 4765- and 1720 MHz in both targets.

2 OBSERVATIONS AND DATA REDUCTION

The observations of two star-forming regions Cep A and W75N were carried out with 5 or 6 telescopes of MERLIN. 4765-MHz OH transition from Cep A was observed in three sessions between 1999 January and March and from W75N in April 2000 (Table 1). Observations of the 1720-MHz OH line towards Cep A were made at two epochs (Table 1). The other ground state transitions were also observed and a comprehensive description of them will appear in a separate paper. Each transition was observed simultaneously in left and right circular polarization (LHC, RHC) and correlated to obtain all four Stokes parameters. The spectral bandwidth of 250-kHz was divided into 128 channels yielding a velocity resolution of 0.12 km s⁻¹ at 4.7 GHz and 0.34 km s⁻¹ at 1720 MHz. The velocity coverage was 16 and 45 km s⁻¹ at 4.7 GHz and 1720 MHz respectively. The band centre was set to a local standard of rest (LSR) velocity of -14 km s⁻¹ for Cep A and 10 km s⁻¹ for W75N.

The phase-referencing technique was applied in all observations, with sources 2300+638 and 2005+403 used as phase calibrators for Cep A and W75N, respectively (Ta-

ble 1). The cycle times between Cep A and its phase reference were 8 min+2 min at the first and second epochs and 3 min+2 min at the third epoch for the 4.7 GHz transition and 6.5 min+2 min for the 1720 MHz transition. For W75N and its phase reference source the cycle time was 3.5 min+2.5 min. The reference sources were too weak to be observed in narrow-band mode, hence they were observed in wide-band (16 MHz) mode to obtain the required signal to noise ratio.

The data reduction was carried out with standard procedures (Diamond et al. 2003) using the local programmes at Jodrell Bank and the Astronomical Image Processing System (AIPS). 3C286 was used as a primary flux density calibrator (Baars et al. 1977) and 3C84 as a point source and bandpass calibrator. The 4.7-GHz data were imaged using a pixel separation of 15-mas and a 40-mas circular Gaussian restoring beam; for the 1720-MHz emission 40-mas pixels and a 120-mas beam were used. In emission-free Stokes *I* maps the rms noise levels (σ) were typically few mJy beam⁻¹ (Table 1). Regions of 15''×15'' and 20''×20'' were searched for emission 4765- and 1720-MHz, respectively. The positions and peak flux densities of maser spots brighter than 10 σ were determined by fitting 2D Gaussian components.

The absolute positional accuracy of maser components measured in the paper was limited by a number of uncertainties: (i) the positional accuracy of the phase calibrators was about 12 mas (Patnaik et al. 1992), (ii) the error arising from uncertainties in telescope positions was about 10 mas (Diamond et al. 2003), (iii) the angular separations between targets and phase calibrators of 2° (Cep A) and 2.8° (W75N) gave errors of 13 mas at 4765 MHz, 30 mas at 1720 MHz for Cep A and 10 mas at 4765 MHz for W75N, taking into account the worst phase-rate for each observation. These combine to give total absolute position errors for maser components in Cep A of 20 and 34 mas at 4765- and 1720 MHz respectively, and of 19 mas for 4765-MHz masers in W75N. Where we are comparing observations using the same phase-reference source and/or the same array, conditions (i) and/or (ii) do not apply and only condition (iii) produces relevant 1 σ systematic position errors. Each maser component also has a relative position error, given approximately by beamsize/signal-to-noise-ratio, but this was negligible, being < 0.5-mas for a typical component.

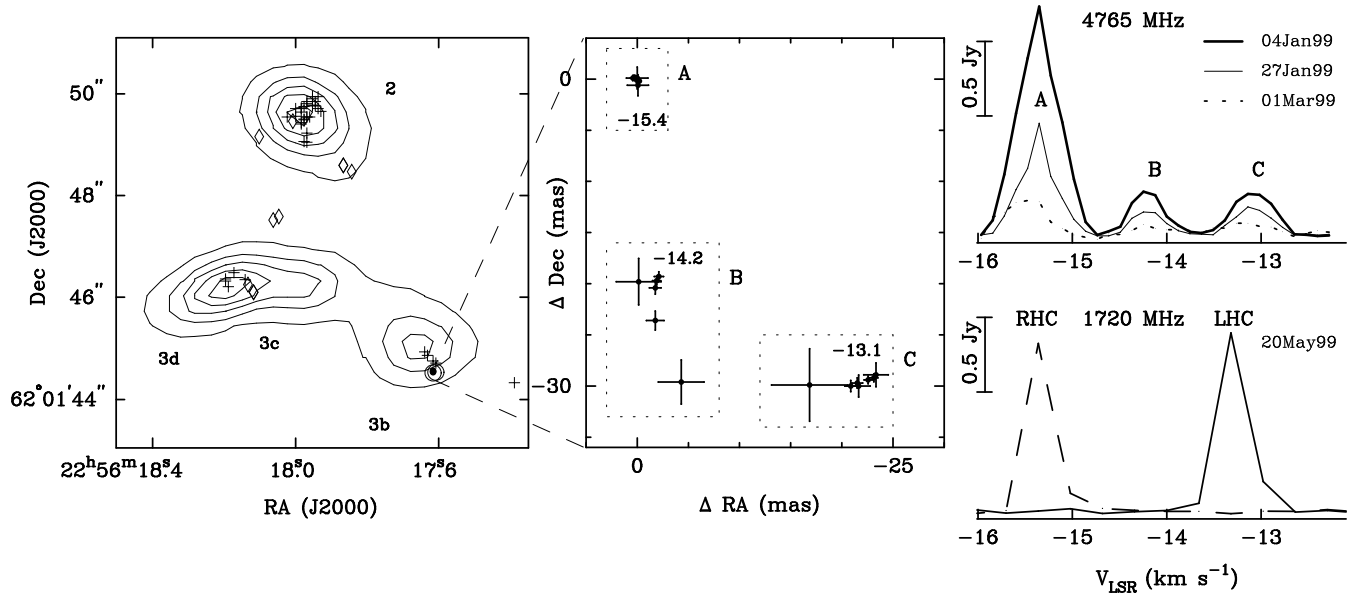


Figure 1. *Left:* The 4.9-GHz VLA continuum map of the Cep A East central region (Garay et al. 1996) with contours at the levels of 10%, 30%, 50%, 70% and 90% of 4.8mJy beam^{-1} . The labels of continuum sources were taken from Hughes & Wouterloot (1984). The 1720-MHz and 4765-MHz OH maser components reported in this paper are shown as circles and dots respectively. The positions of the 22-GHz H₂O maser components (crosses) taken from Torrelles et al. (1998) and those of the 1665-MHz OH maser components (diamonds) (Argon et al. 2000) are overlaid. *Middle:* Distribution of 4765-MHz OH masers relative to the strongest component observed on 1999 January 4. Each of the three groups of components are labelled by the central velocity V_{LSR} (km s^{-1}). The bars indicate the relative errors in maser component positions. *Right:* The *I* Stokes spectra of the 4765-MHz emission at three epochs (top) and the 1720-MHz spectrum in left and right circular polarization (bottom) from Cep A.

Table 2. Components of the 4765-MHz OH maser observed towards Cep A at three epochs. The ΔRA and ΔDec are given relative to the position of the brightest component at the first epoch, i.e. $\text{RA}(\text{J2000}) = 22^{\text{h}}56^{\text{m}}17^{\text{s}}.6176$; $\text{Dec}(\text{J2000}) = 62^{\circ}01'44''.567$.

Epoch	04Jan99			27Jan99			01Mar99			Group
V_c (km s^{-1})	ΔRA (mas)	ΔDec (mas)	S_{4765} (Jy b^{-1})	ΔRA (mas)	ΔDec (mas)	S_{4765} (Jy b^{-1})	ΔRA (mas)	ΔDec (mas)	S_{4765} (Jy b^{-1})	
-15.84	-0.1(1.0)	-0.6(1.0)	0.105				-0.3(3.1)	-3.3(3.3)	0.133	A
-15.72	0.4(0.3)	0.1(0.3)	0.042	-0.1(0.5)	-0.4(0.5)	0.127	-1.8(2.3)	0.1(2.2)	0.166	A
-15.60	0.1(0.1)	0.1(0.1)	0.841	0.0(0.2)	0.0(0.2)	0.305	-2.1(1.9)	0.4(1.9)	0.227	A
-15.47	0.2(0.1)	0.1(0.1)	1.225	0.4(0.2)	0.0(0.2)	0.446	0.1(1.7)	0.3(1.6)	0.235	A
-15.35	0.0(0.1)	0.0(0.1)	1.554	0.0(0.1)	0.0(0.1)	0.744	0.9(1.7)	0.0(1.6)	0.231	A
-15.23	0.3(0.1)	0.2(0.1)	1.109	-0.1(0.2)	0.0(0.2)	0.387	1.1(6.3)	-1.6(7.0)	0.073	A
-15.11	-0.2(0.2)	-0.2(0.2)	0.772	0.0(0.3)	0.1(0.3)	0.241				A
-14.98	0.1(0.3)	-0.1(0.2)	0.378	-0.1(0.6)	-0.6(0.6)	0.095				A
-14.86	0.0(1.0)	0.1(0.3)	0.096							A
-14.49	-0.1(2.2)	-19.8(2.3)	0.058							B
-14.37	-1.8(0.6)	-20.4(0.6)	0.216	-3.7(0.6)	-15.9(0.6)	0.111				B
-14.25	-1.9(0.4)	-19.7(0.4)	0.304	-1.1(0.4)	-18.4(0.4)	0.151	-4.9(5.9)	-23.2(6.9)	0.074	B
-14.12	-2.1(0.5)	-19.3(0.5)	0.274	-2.1(0.5)	-17.3(0.5)	0.147	-2.8(6.2)	-18.7(6.4)	0.048	B
-14.00	-1.8(0.9)	-23.6(0.9)	0.136	-6.3(1.0)	-18.2(1.0)	0.071				B
-13.88	-4.3(2.2)	-29.6(2.2)	0.055							B
-13.51	-16.8(3.7)	-29.9(3.5)	0.033							C
-13.39	-23.3(1.2)	-28.9(1.2)	0.104	-24.6(1.0)	-17.3(0.5)	0.069	-22.4(6.3)	-26.0(8.9)	0.049	C
-13.26	-21.5(0.5)	-29.7(0.5)	0.236	-18.3(0.5)	-28.4(0.5)	0.124	-22.9(6.1)	-28.7(6.5)	0.072	C
-13.14	-22.6(0.4)	-29.4(0.4)	0.290	-19.5(0.4)	-29.9(0.3)	0.197	-18.5(4.7)	-27.8(5.0)	0.076	C
-13.02	-23.1(0.4)	-29.2(0.4)	0.295	-21.0(0.4)	-30.2(0.4)	0.177	-24.9(6.0)	-28.1(6.4)	0.062	C
-12.89	-20.9(0.6)	-30.0(0.5)	0.221	-19.5(0.6)	-30.1(0.5)	0.119				C
-12.77	-21.6(1.0)	-30.0(1.0)	0.106	-22.4(1.3)	-30.0(1.2)	0.056				C

Table 3. Components of the 1720-MHz OH maser detected from Cep A on 1999 May 20. The Δ RA and Δ Dec are given similarly as in Table 2.

V_c (km s^{-1})	Δ RA (mas)	Δ Dec (mas)	S_{1720} (Jy b^{-1})	Polzn.
-15.36	-20.2 (0.4)	-50.0 (0.4)	1.122	RHC
-15.02	-20.4 (4.0)	-49.7 (4.0)	0.121	RHC
-13.66	-45.7 (9.0)	-23.2 (9.0)	0.059	LHC
-13.32	-36.5 (0.4)	-33.7 (0.4)	1.050	LHC
-12.98	-37.8 (2.8)	-33.0 (3.0)	0.210	LHC

3 RESULTS

3.1 Cep A

The results for Cepheus A are summarized in Figure 1 and Tables 2 and 3. The 4765-MHz maser emission was found in the velocity range from -16 to -12.7 km s^{-1} at the S–W edge of the HII region labelled as 3b by Hughes & Wouterloot (1984) (Fig.1). A single unresolved maser component was detected in 22 spectral channel maps at the first epoch, and in fewer channels at subsequent epochs. The velocity, position (with relative errors arising from noise and fitting uncertainties) and flux density of each maser component are given in Table 2 at the three epochs. All components brighter than 10σ are included. At all three epochs the spectrum showed three features separated by about 1.1 km s^{-1} from each other, with the strongest emission near -15.4 km s^{-1} (Fig.1). The emission comes from a region about 40 mas in size, with three groups of maser components labelled A, B and C in Fig.1 that correspond to the three spectral features. A is a single maser spot and B and C spots have angular sizes of the order of about 10 mas. Each group has a well defined central velocity. There is an overall velocity gradient along the arc-like structure from the north (blue-shifted emission) to the south west (red-shifted emission). This structure was stable at all three epochs. At the first epoch the strongest 4765-MHz feature had a peak brightness of $1.55 \text{ Jy beam}^{-1}$, corresponding to a lower limit on the brightness temperature of $7 \times 10^7 \text{ K}$. The peak flux density S_{4765} of all three features showed a clear decrease over the time span of 8 weeks that can be modelled as

$$S_{4765} \sim t^\beta \quad (1)$$

where t is the time in days since the start of the MERLIN observations. For all three features the mean value of β was -0.34 ± 0.08 .

We fitted a single Gaussian component to all spectral features, obtaining full width at half maximum intensity (FWHM) values ranging from 0.38 km s^{-1} to 0.82 km s^{-1} . However, we did not find any relation between the peak flux density and the FWHM.

There was no difference between LHC and RHC polarization of the 4765-MHz maser emission within 10σ . Data from the first epoch were inspected for linearly polarized features and no emission was found to a limit of about 8 mJy. At the third epoch we detected neither 4660-MHz nor 4750-MHz emission above a level of 20 mJy over the whole region searched. Therefore, the upper limits for the integrated flux density ratios between three 6-cm OH lines were $S(i)_{4660} : S(i)_{4765} \leq 0.19$ and $S(i)_{4750} : S(i)_{4765} \leq 0.18$.

1720-MHz maser emission was found at both epochs of observation. The parameters of components detected at the first epoch (above the 10σ noise level) are given in Table 3. The emission appeared as right and left completely circularly polarized features separated by 2.1 km s^{-1} (Fig.1). These components coincided within 23 mas in the sky so that there is no doubt that they are a Zeeman pair. The central velocity of -14.34 km s^{-1} was close to the central velocity of the 4765-MHz feature B. Assuming that the 1720-MHz emission comes from well-separated σ^{+1} and σ^{-1} components, with a line splitting of $118 \text{ km s}^{-1} \text{ G}^{-1}$, we estimate a magnetic field strength of -17.3 mG in the maser region. It is striking that the 1720-MHz emission coincided with group B of the 4765-MHz maser components within 40 mas. Both lines were detected at a position not previously noted for OH maser emission. Moreover, within an area of size $2'' \times 2''$ centred at the strongest component of group B we did not detect any emission in the other three ground state OH lines above a sensitivity level of 15 mJy. The 1720-MHz component had a peak brightness of $1.12 \text{ Jy beam}^{-1}$, corresponding to a lower limit on the brightness temperature of $5 \times 10^7 \text{ K}$. 1720-MHz emission was also detected on 1999 June 16 within the same velocity range and at the same positions, but we did not analyse these data because the emission was too weak for self-calibration, being only half the intensity observed on 1999 May 20.

3.2 W75N

Results for W75N are summarized in Figure 2 and Table 4. W75N showed a complex OH spectrum at 4765 MHz with three features within a velocity range of only 1.1 km s^{-1} (Fig.2). The maser components found are listed in Table 4 where the velocities, relative positions and the flux densities are given. The 4765-MHz components are located on the S–W edge of the HII region mapped in the radio continuum and labelled as Ba by Hunter et al. (1994) or VLA 1 by Torrelles et al. (1997) (Fig.2). 4765-MHz OH emission was detected from three regions A, B and C located in a chain of length comparable to the synthesised beam size and roughly along the N–S direction (Fig.2). There is a clear velocity gradient from the north (blue-shifted) to the south (red-shifted). The brightest component had a peak brightness of $1.96 \text{ Jy beam}^{-1}$, corresponding to a lower limit on the brightness temperature of $1.0 \times 10^8 \text{ K}$. The position of the 4765-MHz maser structure coincides to within 60 mas with the position of the 1720-MHz Zeeman pair Z_6 reported by Hutawarakorn et al. (2002), while the demagnetized velocity of the 1720-MHz Zeeman pair of 9.4 km s^{-1} is very close (0.3 km s^{-1}) to the velocity of feature A of the 4765-MHz profile (Fig.2). This implies that both maser transitions arise from the same region and suggests similar pumping conditions.

4 DISCUSSION

The important conclusion that can be inferred from the MERLIN observations of the two targets is that the 4765-MHz and 1720-MHz masers appear within the same velocity ranges and coincide in the sky well within the position uncertainties. This finding is especially valuable for Cep A as

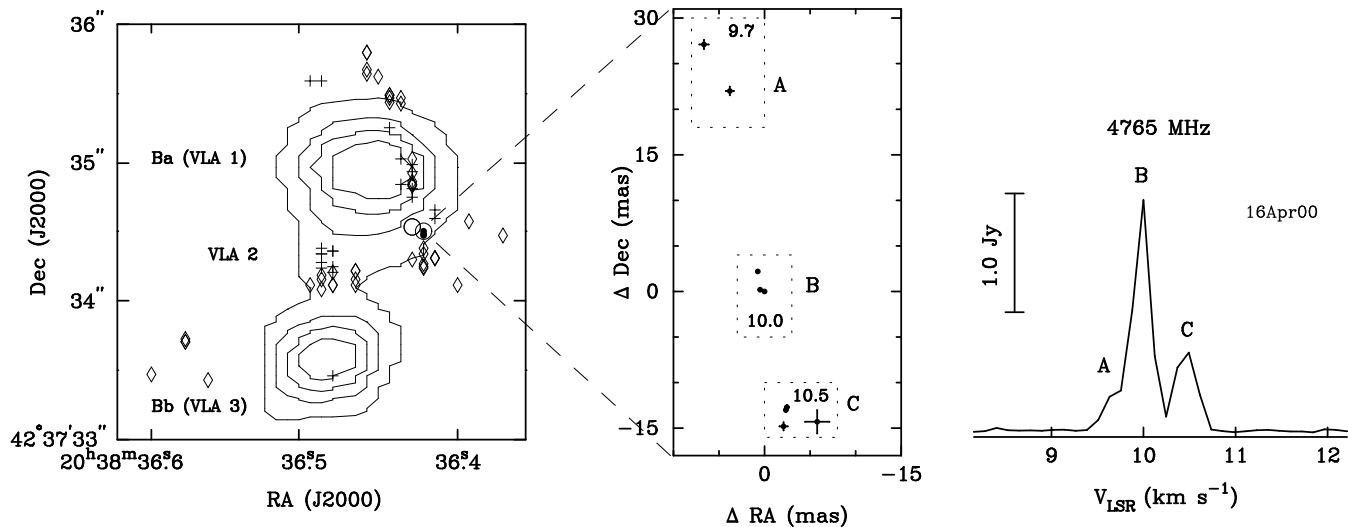


Figure 2. *Left:* The map of the 8.4-GHz continuum emission of the W75N region (Hunter et al. 1994). The contours correspond to 10%, 30%, 50% and 70% of 2.5 mJy beam⁻¹. The 4765-MHz masers are marked by dots. Open circles and diamonds indicate the positions of the OH 1720-MHz and 1665-MHz masers respectively (Hutawarakorn et al. 2002), while crosses mark 22-GHz H₂O masers (Torrelles et al. 1997). *Middle:* Relative positions of OH 4765-MHz masers. The central velocity V_{LSR} km s⁻¹ of each group and relative position errors of components are given. *Right:* The total flux density spectrum of the OH 4765-MHz emission from W75N.

Table 4. Components of OH 4765-MHz transition found in W75N. The J2000 coordinates of the brightest component are RA = 20^h38^m36^s.4238; Dec = 42°37'34".484.

V_c (km s ⁻¹)	Δ RA (mas)	Δ Dec (mas)	S_{4765} (Jy b ⁻¹)	Group
9.63	6.6(0.5)	27.1(0.5)	0.270	A
9.75	3.8(0.4)	22.0(0.5)	0.316	A
9.88	0.7(0.1)	2.2(0.1)	0.980	B
10.00	0.0(0.1)	0.0(0.1)	1.957	B
10.12	0.5(0.2)	0.2(0.2)	0.594	B
10.25	-5.8(1.3)	-14.3(1.3)	0.104	C
10.37	-2.5(0.2)	-12.7(0.2)	0.512	C
10.49	-2.3(0.2)	-13.0(0.2)	0.630	C
10.62	-2.1(0.5)	-14.8(0.5)	0.272	C

the observations of the two transitions were carried out at two epochs only 2.5 months apart. For this source the position of group B of the 4765-MHz components differs by less than 40 mas from that of the 1720-MHz emission, while the central velocities of features at both transitions do not differ by more than 0.14 km s⁻¹. It is therefore highly probable that the 4765- and 1720-MHz lines originate in the same gas volume.

The flux density at 4765 MHz decayed with time as given by Equation 1 using $\beta = -0.34 \pm 0.08$ (Section 3.1). This gives an extrapolated flux density of 45 mJy on 1999 May 20, the epoch of the 1720-MHz observation. This implies a ratio of ~ 25 (± 5) between the peak flux densities at 1720 and 4765 MHz. Such an intensity ratio can be explained using the model by Gray et al. (1991) if there is no overlap between the pump line transitions for the different maser lines, assuming far infrared pumping. This occurs for regions with an H₂ number density, n_{H_2} , of 4×10^6 cm⁻³ and an OH number density, n_{OH} , of 2×10^2 cm⁻³ over a wide kinetic temperature range from 100 – 200 K. If there is a

large-scale velocity field of up to 1.7 km s⁻¹ across the masing region, line overlap allows the 1720-MHz maser to survive to higher densities with n_{H_2} up to a few $\times 10^7$ cm⁻³.

Under similar conditions saturated gain is predicted at both 1720- and 4765-MHz, as shown in Fig.12 of Gray et al. (1992). Their model also predicts the absence of the main line ground state OH masers and the other two 4.7-GHz lines. This is fully consistent with our observations: no emission was detected at 1665 or 1667 MHz, with a typical rms of 5 mJy in a projected area $2'' \times 2''$ centred at feature B of the 4765-MHz emission (Niezurawska et al., in prep.). Moreover, our upper limits to emission at 4660- and 4750 MHz show that the 4765-MHz emission is at least 5 times stronger. We note that the gain length of the 4765-MHz emission calculated by Gray et al. (1992) is of the same order as the projected linear size of 4×10^{14} cm of maser structure in Cep A for the assumed distance of 725 pc.

Our lower limit for the brightness temperature of 4765-MHz masers of 7×10^7 K in Cep A does not preclude saturation. Very Long Baseline Interferometry observations of W3(OH) and two other star forming regions have revealed angular sizes of 4765-MHz components as small as a few mas, implying brightness temperatures up to 10^9 K (Baudry et al. 1988; Baudry & Diamond 1991) which can be reached due to saturated amplification. The relationship between the linewidth and the peak flux density for feature A established from single-dish observations (Szymczak et al. 2000) appears to be consistent with a model of saturated maser emission.

The newly detected 1720/4765-MHz OH maser components in Cep A are located $2''.8$ to the south-west of the previously known clusters of 1665- and 1667-MHz masers observed by Cohen et al. (1984); Migenes et al. (1992) and Argon et al. (2000). Comparison with the 1.3-cm continuum map reported by Torrelles et al. (1998) reveals that our OH masers lie about $0''.5$ to the S-W of the centre of the weak (2.3 mJy) continuum source (labelled as 3b in Fig.1) elongated

gated at a position angle of about 50° . They are accompanied by four weak (<0.3 Jy) 22-GHz H_2O maser components grouped in a velocity range from -14.8 km s^{-1} to -12.8 km s^{-1} and aligned almost parallel to the source axis. Not obvious velocity gradient is seen along the water maser emission (Torrelles et al. 1998). The 1720/4765-MHz masers lie just at the S–W edge of this structure $0''.16$ from the nearest -12.8 km s^{-1} water component.

The overall arc-like structure of the 4765-MHz maser in Cep A has a projected size of 4×10^{14} cm and shows a velocity gradient along the axis of continuum source 3b, with a velocity dispersion of 3.1 km s^{-1} . The adjacent 22-GHz water components exhibit a velocity dispersion of 2 km s^{-1} over a projected size of 4×10^{15} cm. These data clearly suggest a kinetically complex medium where the velocity field may be dominated by turbulence (e.g. Field 1982). The presence of turbulence in Cep A has also been demonstrated by proper motion studies (Migenes et al. 1992).

The source labelled 3b in Fig.1 is characterized by a flat spectral index between 1.5-GHz and 15-GHz indicative of optically thin thermal emission (Garay et al. 1996) which may arise from shock heated gas excited by an external source. The adjacent sources 2, 3c and 3d show positive spectral indices α (convention $S \propto \nu^\alpha$) suggesting an internal source of energy. It has been postulated that source 3b may be at the earliest evolutionary stage among these four sources (Torrelles et al. 1998). However, our detection of the 1720/4765-MHz masers does not support that. The presence of weak H_2O masers (Torrelles et al. 1998) and OH masers in two lines has been interpreted as being due to object 3b being ionised by an embedded B2 ZAMS star (Garay et al. 1996). If source 3b harbours a star then for the assumed distance of 725 pc the excited OH masers arise at a projected separation of 5×10^{15} cm. The edge of the molecular cloud, where $n_{\text{H}_2} \sim 2 \times 10^4$ cm^{-3} , hosts a magnetic field of strength $B = 0.3$ mG, which scales with number density as $B \sim n^{0.4-0.5}$ (Garay et al. 1996 and references therein), consistent with compression of the interstellar magnetic field during star formation. Our measurements of 1720-MHz Zeeman splitting (Section 3.1) imply a magnetic field strength of at least 17.3 mG in the OH maser region. This leads to an estimate of $n_{\text{H}_2} \simeq 7 \times 10^7$ cm^{-3} . This value agrees well with the theoretical prediction for the 1720-/4765-MHz masers (Gray et al. 1992).

The 4765-MHz emission from Cep A showed pronounced variability, decreasing by a factor of 4 over a period of 7 weeks. The MERLIN data are consistent with single dish data previously reported by Szymczak et al. (2000), assuming that feature A corresponds to the peak discovered in the single-dish observations. More recent data taken with the Toruń antenna suggest the maser flux density continues to decline to 0.2 Jy or below (Fig.3). The temporal characteristic of the 4765-MHz emission of Cep A seem to resemble that observed in Mon R2 (Smits et al. 1998).

It seems that the 1720-MHz maser also varies on a time scale of weeks. It is remarkable that Cep A showed no 1720-MHz emission for many years throughout the 1980's, with upper limits of 0.1 to 0.3 Jy being regularly observed (e.g. Cohen, Brebner & Potter 1990). The emission turned on some time between July 1994, when the upper limit was 0.3 Jy (Mashedier & Cohen, in preparation), and June 1995, when a pair of emission features appeared at ~ 2 Jy with

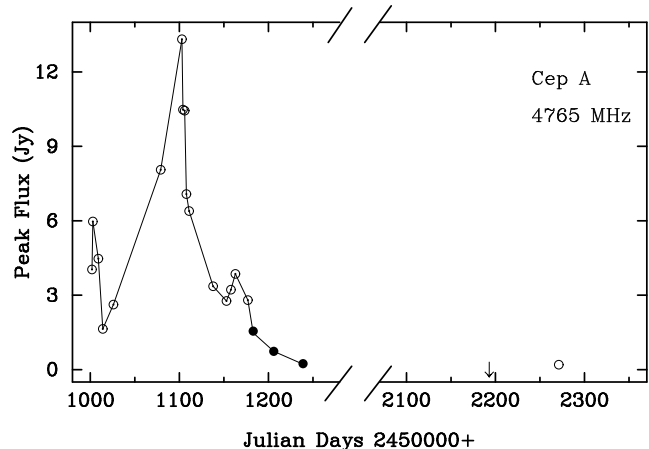


Fig. 3. Variability of the strongest feature (A) of the 4765-MHz line in Cep A over the period from 1998 July 07 to 2001 December 27. The open circles correspond to the single dish data (Szymczak et al. 2000) and unpublished observations, the arrow marks an upper limit, and dots represent the MERLIN data analysed in this paper.

velocities of -15.9 and -13.9 km s^{-1} (Cohen, unpublished data).

The 4765-MHz maser emission discovered towards W75N coincides in velocity (<0.1 km s^{-1}) and position (<60 mas) with the 1720-MHz maser mapped with MERLIN about 6.5 years earlier by Hutawarakorn et al. (2002), the Zeeman pair Z_6 . The 4765-MHz components in W75N are located between two clusters of 1665-MHz OH masers at mean velocities of $V_{\text{LSR}} = 7.3$ km s^{-1} (northern) and $V_{\text{LSR}} = 10.6$ km s^{-1} (southern) labelled as 3 and 4 by Baart et al. (1986). The 22-GHz H_2O masers at 10.7 km s^{-1} and 12.6 km s^{-1} reported by Torrelles et al. (1997) lie about ~ 200 mas north of the group B of 4765-MHz maser emission. The 1720-/4765-MHz components of W75N are projected at the S–W edge of the HII region labelled Ba (VLA1) by Hunter et al. (1994), which has a spectral index of about 0.7 between 8.5-GHz and 22-GHz. This indicates partially optically thick emission from an ionized biconical jet (Torrelles et al. 1997). The 1720-/4765-MHz masers lie at the S–W edge of a molecular outflow at distance of $0''.54$ from the centre of the 22-GHz continuum emission. For the assumed distance of W75N of 2 kpc the projected distance of the 1720-/4765-MHz masers from a central star is 1.6×10^{16} cm.

The OH maser emission from W75N has been modelled in detail by Gray, Hutawarakorn & Cohen (2003). Their model predicts 4765-MHz emission from $+7$ to $+12$ km s^{-1} and 1720-MHz emission from $+12$ to $+13$ km s^{-1} (Figs. 4 and 5 in that paper), in good agreement with the velocities and positions found here. The physical conditions in the region where 1720-MHz and 4765-MHz coincide in the model are as follows: $n_{\text{H}_2} = 5 \times 10^8$ cm^{-3} , $n_{\text{OH}} = 5 \times 10^3$ cm^{-3} , kinetic temperature $T_{\text{K}} = 9.7$ K, dust temperature $T_{\text{d}} = 45$ K. These are much denser and colder than the conditions thought to prevail in the typical OH-HII region W3(OH) where the amplification paths are much longer, the OH masers are much more powerful and intense, and are thought to lie in a shocked molecular envelope surrounding the expanding HII region. In W75N the molecular gas is cooler and denser and is associated with a rotating molecular disc

and bipolar outflow, at an earlier evolutionary phase than W3(OH).

In both sources we found the association of 1720- and 4765-MHz OH masers that strongly supports the model by Gray et al. (1992). In contrast, the modelling of Pavlakis & Kylafis (1996a); Pavlakis & Kylafis (1996b) and Cragg et al. (2002) poorly fits our data.

A strong association between 4765- and 6035-MHz OH transitions has been reported recently by Dodson & Ellingsen (2002). The 6031- and 6035-MHz OH masers were detected towards Cep A in a velocity range from -10 to -8 km s^{-1} (Baudry et al. 1997). Towards W75N they found only the 6035-MHz emission in a velocity range from 7 to 8 km s^{-1} . These data imply that in both sources the 6031-/6035-MHz masers do not coincide in velocity with the 1720-/4765-MHz masers. No information is available where the 6031-/6035-MHz masers are located.

5 CONCLUSIONS

Two star-forming regions Cep A and W75N have been mapped in the 4765- and 1720-MHz maser lines. Components of the excited OH emission at 4765 MHz form arc and linear structures of projected size $4 \times 10^{14} - 1 \times 10^{15} \text{ cm}$ with a very well defined velocity gradient. These structures lie at projected distances of $0.5 - 2 \times 10^{16} \text{ cm}$ from the central star and its surrounding H II region. In both sources the two maser lines show a good spatial coincidence within the uncertainty of $\sim 35 \text{ mas}$ and demagnetised velocity pairing within the 0.2 km s^{-1} spectral resolution, implying that the 4765-/1720-MHz masers originate from the same gas volume. No emission of any other 1.6- and 4.7-GHz OH transitions was found in these regions. Including the present data there are now three examples of co-propagating 1720-MHz and 4765-MHz masers, where the positional association has been verified to within ~ 30 milliarcseconds.

ACKNOWLEDGMENTS

The authors thank Dr. M. Gray for discussions and Dr. G. Garay and Dr. T. Hunter for making available the continuum maps of Cep A and W75N. MERLIN is a national facility operated by the University of Manchester at Jodrell Bank on behalf of PPARC. AN acknowledges a fellowship funded by the EU under the Marie Curie Training Site programme. The work was supported by grant 2P03D01122 of the Polish State Committee for Scientific Research.

REFERENCES

- Argon A.L., Reid M.J., Menten K.M., 2000, *ApJS*, 129, 159
 Baars J.W.M., Genzel R., Pauliny-Toth I.I.K., Witzel A., 1977, *A&A*, 61, 99
 Baart E.E., Cohen R.J., Davies R.D., Norris R.P., Rowland P.R., 1986, *MNRAS*, 219, 145
 Baudry A., Desmurs J.F., Wilson T.L., Cohen R.J., 1997, *A&A*, 325, 255
 Baudry A., Diamond P.J., 1991, *A&A*, 247, 551
 Baudry A., Diamond P.J., Booth R.S., Graham D., Walmsley C.M., 1988, *A&A*, 201, 105
 Blaauw A., Hiltner W.A., Johnson H.L., 1959, *ApJ*, 130, 69
 Cohen R. J., 1989, *Rep.Prog.Phys.*, 52, 881
 Cohen R.J., Brebner G.C., Potter M.M., 1990, *MNRAS*, 246, 3P
 Cohen R.J., Mashedier M.R.W., Caswell J.L., 1995, *MNRAS*, 274, 808
 Cohen R.J., Mashedier M.R.W., Walker R.N.F., 1991, *MNRAS*, 250, 611
 Cohen R.J., Rowland P.R., Blair M.M., 1984, *MNRAS*, 210, 425
 Cragg D.M., Sobolev A.M., Godfrey P.D., 2002, *MNRAS*, 331, 521
 Diamond P.J., Garrington S.T., Gunn A.G., Leahy J.P., McDonald A., Muxlow T.W.B., Richards A.M.S., Thomasson P., 2003, *MERLIN User Guide*, ver. 3
 Dickel J.R., Dickel H.R., Wilson W.J., 1978, *ApJ*, 223, 840
 Dodson R.G., Ellingsen S.P., 2002, *MNRAS*, 333, 307
 Field D., 1982, *MNRAS*, 201, 527
 Garay G., Ramirez S., Rodriguez L.F., Curiel S., Torrelles J.M., 1996, *ApJ*, 459, 193
 Goetz J.A., Pipher J.L., Forrest W.J., Watson D.M., Raines S.N., Woodward C.E., Greenhouse M.A., Smith H.A., Hughes V.A., Fischer J., 1998, *ApJ*, 504, 359
 Gray M.D., Cohen R.J., Richards A.M.S., Yates J.A., Field D., 2001, *MNRAS*, 324, 643
 Gray M.D., Doel R.C., Field D., 1991, *MNRAS*, 252, 30
 Gray M.D., Field D., Doel R.C., 1992, *A&A*, 262, 555
 Gray M.D., Hutawarakorn B., Cohen R.J., 2003, *MNRAS*, 343, 1067
 Hughes V.A., Cohen R.J., Garrington S., 1995, *MNRAS*, 272, 469
 Hughes V.A., Wouterloot J.G.A., 1984, *ApJ*, 276, 204
 Hunter T.R., Taylor G.B., Felli M., Tofani G., 1994, *A&A*, 284, 215
 Hutawarakorn B., Cohen R.J., Brebner G.C., 2002, *MNRAS*, 330, 349
 Migenes V., Cohen R.J., Brebner G.C., 1992, *MNRAS*, 254, 501
 Palmer P., Gardner F.F., Whiteoak J.B., 1984, *MNRAS*, 211, 41p
 Patnaik A.R., Browne I.W.A., Wilkinson P.N., Wrobel J.M., 1992, *MNRAS*, 254, 655
 Pavlakis G.K., Kylafis N.D., 1996a, *ApJ*, 467, 300
 Pavlakis G.K., Kylafis N.D., 1996b, *ApJ*, 467, 309
 Smits D.P., 2003, *MNRAS* 339, 1
 Smits D.P., Cohen R.J., Hutawarakorn B., 1998, *MNRAS*, 296, L11
 Szymczak M., Kus A.J., Hrynek G., 2000, *MNRAS*, 312, 211
 Torrelles J.M., Gomez J.F., Garay G., Rodriguez L.F., Curiel S., Cohen R.J., Ho P.T.P., 1998, *ApJ*, 509, 262
 Torrelles J.M., Gomez J.F., Rodriguez L.F., Ho P.T.P., Curiel S., Vazquez R., 1997, *ApJ*, 489, 744